Influence of Various Relative Humidity and Chloride Concentrations on Probability of Corrosion for Reinforced Concrete Members: A Review

Mostafa Hassan[1*]

[1]*Construction and Building Engineering Department, Arab Academy for Science, Technology, and Maritime Transport- AASTMT, Abu Qir Campus, Alexandria, 1029,Egypt.*

Corresponding Author[*]*: Mostafa Hassan, hassan92mostafa@yahoo.com*

Abstract: Chloride-induced corrosion is a severe form of corrosion for vital reinforced concrete (RC) structures subjected to extreme climate change, compared to carbonation-induced corrosion.This research aims to determine the influence of various environmental variables on chloride-induced corrosion, in terms of the reliability, durability, and service life of RC structures. This research employs the Monte Carlo Simulation method to evaluate the probability of corrosion initiation (PCI) under future climate scenarios for a North American province. The average diffusion coefficient of chloride ions in concrete considers the influence of maximum temperature and relative humidity levels. The PCI is evaluated at different concrete covers and chloride concentrations at two Representative Concentration Pathways for the low emission scenario (RCP2.6) and high emission scenario (RCP8.5). The results of this research indicate that as the concrete cover for the RC deck increased beyond 70 mm instead of 30 or 40 mm, there was a marked reduction in PCI across all RCPs and humidity levels, confirming the protective effect of a thicker concrete layer. This study provides valuable insights into the assessment and management of RC bridges under climate change and offers a predictive model for assessing the risk of corrosion for RC decks.

Keywords: Climate change, Chloride-induced corrosion, Concrete cover, Maximum Temperature, Relative humidity level, Probability of corrosion.

1. Introduction

Chloride-induced corrosion is an electrochemical process initiated when chloride ions penetrate the concrete cover, leading to the breakdown of the protective layer around steel rebars [1-7]. This breakdown allows moisture and oxygen to reach the steel surface, resulting in expansion and cracking as corrosion by-products accumulate. The use of supplementary materials, such as fly ash (FA) and slag (SG), in concrete mixes has shown promise in reducing chloride penetration, thereby enhancing the durability and safety ofreinforced concrete (RC) structures. Hassaan et al.[8], Hassaan et al. [9], and Hassaan et al. [10] showed that the effect of cracks increases the rate of corrosion in heavyweight concrete.

RC bridges are vital components of infrastructure systems, yet the impacts of climate change increasingly threaten their durability. Rising CO_2 emissions, fluctuating temperatures, and the increased use of deicing salts have been identified as key contributors to accelerated deterioration, particularly through chloride-induced corrosion. There is an urgent need for a comprehensive, climate-sensitive approach to assess and manage the durability of RC bridges, ensuring their resilience against the evolving threat of climate change. Chloride ions can penetrate the concrete cover through different transport mechanisms, such as diffusion, absorption, permeation, convection, and dispersion [11, 12]. The convection is driven by the moisture gradient in concrete, and permeation occurs due to hydrostatic pressure. Moreover, adsorption occurs in concrete surface layers that are subjected to wetting and drying cycles, and it only affects the exposed concrete surface down to 10-20 mm. Chloride diffusion (i.e., concentration gradient) is a transfer of free chloride ions by random motion in the pore solution, resulting in a net flow from higher to lower concentration regions. The various factors influencing chloride ion transmission to the concrete microstructure are explained in detail, as shown in Table 1. The rate of chloride ingress is proportional to the concentration gradient and the diffusion coefficient of the concrete according to Fick's first law of diffusion [13]. When chlorides reach the steel rebars, they can break the protective passive film around the steel rebars, making them susceptible to corrosion. This will lead to the formation of corrosion products that occupy a larger volume than the original steel; as a result, expansive pressures are generated within the concrete, leading to the generation of cracks inside the concrete structure. Free chloride is responsible for the reinforcement corrosion. The bound chloride either is physically adsorbed within the pores or chemically reacts with the hydrated products. Chloride binding in concrete affects the rate of chloride ingress, which in turn determines the initiation of chloride-induced corrosion.

Table 1.Influencing factors affecting chloride ion transmission in concrete microstructure.

Factors for chloride ion transmission in concrete	Discussion
1. Water-Cement Ratio	A higher water-cement ratio will increase the porosity, which directly leads to the acceleration of the chloride migration rate in concrete. The relationship between chloride diffusivity and the water-cement ratio (W/C) in the OPC concrete is shown in equation (1). $D_{28} = 10^{-12.06+\left(2.4\times\frac{W}{C}\right)}$ (1) Where D_{28} is the chloride ion diffusivity (m^2/s).
2. Exposure Time	The diffusion rate for chloride ions in cementitious material is related to cement hydration and time.Thomas and Bamforth [14] developed the relationship between chloride diffusivity and time of chloride exposure, as shown in equation (2), based on the age factor. $f_t = \left(\frac{t_o}{t}\right)^m$ (2) Where: f_t is the parameter considering the effect of time on chloride migration; (t_o) is the reference time, $t_o = 28$ days, according to Engelund et al. [15].
3. Chloride Ion Binding Effect	Binding chloride is developed by the chemical binding of cement hydration. The total chloride content is equal to the free chloride content and the chloride binding content, as shown in equation (3). $C_t = w_e C_f + C_b$ (3) Where: C_t is the total chloride content (%); C_f is the free chloride content (%); C_b is the content of bound chloride (%); w_e is the ratio of the volume of evaporable pore to the concrete volume, generally taking 8%. It is important to consider the effect of chloride binding as follows: (1) Only free chlorides are responsible for the corrosion of steel rebars [16], (2) The chemical binding of chloride ions with C_3A and C_4AF results in the formation of calcium chloroaluminate hydrate, which is known as Friedel's salt, which has a less porous structure and slows down the transport of chloride ions, as shown in equations (4) and (5). $Ca(OH)_2 + 2\ NaCl \rightarrow Ca\ Cl_2 + 2\ Na + 2\ OH$ (4)

	$C_3A + CaCL_2 + 10H_2O \rightarrow C_3A.CaCl_2.10\ H_2O$ (5)
4. Maximum Temperature	The corrected chloride diffusion coefficient, which includes the effect of the temperature $f_1(T)$, the equivalent maturation time $f_2(t_e)$, and relative humidity$f_3(RH)$, is studied in various research [3, 5] based on equation (6). $D_c = D_m \times f_1(T) \times f_2(te) \times f_3(RH)$ (6) Where D_m (m^2/s) and D_c (m^2/s) are the average chloride diffusion coefficient and the corrected chloride diffusion coefficient changing over time. Temperature significantly affects chloride ion diffusion. High temperatures accelerate chloride diffusivity and reduce chloride binding capacity (see equation (7)). $f_t = \exp\left[\frac{U}{G} \times \left(\frac{1}{T_o} - \frac{1}{T}\right)\right]$ (7) Where: f_T is the temperature coefficient on chloride diffusion coefficient; T is the ambient temperature (℃); T_o is the initial temperature (℃), G is the ideal gas constant, 8.314 J/(mol K^{-1}); U is the activation energy in the diffusion process, and its values are based on W/C ratio according to Page et al.[17].
5. Relative Humidity	Bazant and Najjar [18] proposed the effect coefficient (f_{RH}) of relative humidity on chloride migration (see equation (8)). $f_{RH} = \left[1 + \left(\frac{1 - RH}{1 - RH_c}\right)^4\right]^{-1}$ (8) Where: RH is the relative humidity (%); RH_c is the critical relative humidity (75%).

Chloride-induced corrosion of steel rebars in RC members is one of the primary causes of deterioration in North American infrastructure. Bridges and parking garages exposed to de-icing salts are particularly vulnerable, with the damage manifesting as cracking and spalling of the concrete cover. Chloride ingress leads to steel rebar corrosion, which weakens the structural integrity of RC bridges [19]. In Canada, the economic impact of corrosion on RC infrastructure is also significant, due to corrosion-related deterioration. Upgrading Canada's distressed infrastructure, particularly in road transportation and water systems, is estimated to require a substantial financial commitment. As of the latest data, according to Statistics Canada in 2023, the total cost of replacing road and water infrastructure in poor or very poor condition is estimated to exceed $350 billion. This estimate emphasizes these critical sectors' substantial wear and funding deficit over time. This ongoing challenge highlights the need for substantial investment to maintain and upgrade the foundational infrastructure supporting Canada's economy and quality of life. Extreme weather events have caused substantial damage to bridges and culverts, particularly in regions such as Manitoba, Saskatchewan, and the Atlantic provinces. In 2003, Hurricane Juan in the Atlantic region caused extensive damage to infrastructure, with rehabilitation costs reaching 200 million CAD. The impact of climate change on infrastructure accelerates deterioration, increases rehabilitation costs, and reduces serviceability. Reliable service life models are essential for designing resilient structures by helping engineers select appropriate materials and concrete covers that ensure the bridge's design life is met.

The deterioration process of steel rebars corrosion includes the following stages: depassivation of the steel rebars (stage 1), formation of cracks (stage 2), spalling of the concrete cover (stage 3), and collapse of the structure through

either bond failure(stage 4). The first stage is related to chloride-induced corrosion initiation, while the second through fourth stages are related to corrosion propagation due to chlorides. The probability of corrosion for stage 4 is significantly lower than that of stage 1 (depassivation of the reinforcement). The changes in the reliability index and failure probability are marginal from stage 1 to stage 2. The likelihood of corrosion can be investigated by utilizing the Monte Carlo simulation method [1-7].

The resilience of RC structures, particularly bridge members, is fundamental to the integrity of transportation infrastructure. As critical components in supporting the mobility of people and goods, these structures are increasingly threatened by environmental degradation, primarily due to chloride and carbonation-induced corrosion. Climate change intensifies these threats, as rising temperatures and increased CO_2 concentrations accelerate degradation processes, posing long-term risks to infrastructure sustainability and safety. Bridges are critical components of transportation networks, providing essential connectivity and enabling the efficient movement of goods and people.

The reliability-based maintenance management for RC bridge structures encompasses the following components: condition assessment models, probabilistic deterioration prediction models, probabilistic risk assessment models, and maintenance optimization models, as outlined by Lounis and Daigle[20]. The probabilistic deterioration model and risk assessment were developed for the corrosion initiation stage [1-5]. Such probabilistic corrosion initiation models, for chloride-induced corrosion, are necessary steps to address the uncertainties involved in predicting deterioration and managing maintenance.

Incorporating SCMs, such as FA, silica fume (SF), and SG, into concrete mixes can enhance durability [21] (see Table 2). The diffusion rate in concrete using OPC could be reduced to 2-5 times using mineral admixtures, especially SG cement. These materials fill concrete pores and create a denser structure, helping to mitigate corrosion in future climates.

Table 2. Impact of various SCMs on the chloride penetration depth.

SCMs	Chloride Penetration Depth
FA	The addition of FA significantly reduced the penetration of chloride ions into concrete pores [22-24]. Ampadu et al.[25] found that replacing 40% of the cement in the mix with FA yields the best results regarding chloride diffusivity through cement-FA pastes. Using FA will also increase the service life of structures exposed to chlorides.
SF	Utilizing dispersed SF in the concrete mix will result in a dramatic reduction in chloride penetration into concrete pores. Bentz et al. [26] found that replacing SF with 10% OPC would reduce chloride diffusivity by15 times compared to the mix without SF.For concretes exposed to chloride environments, adding SF will significantly increase the service life predicted by the life-365 model [27].A 10% to 20% replacement of micro-silica in cement resulted in a 2 to 11 times reduction in the chloride diffusion coefficient compared to that of OPC concrete, due to the development of secondary calcium silicate hydrate.
SG	SG enhances the resistance of concrete pores to chloride penetration [21,28]. Zhao et al.[21] found that concrete specimens with higher percentages of SG exhibited greater resistance to the combined effects of chloride ion attack and freeze-thaw exposure.

To mitigate the consequences of chloride-induced corrosion in RC structures, specific requirements are recommended in the future:

- Using supplementary cementitious materials (SCMs) in the concrete mix, such as FA, SG, silica fume (SF), etc.
- Providing adequate concrete cover for the reinforcement that satisfies specific minimum requirements according to the standard code (i.e., minimum 50 mm for RC members made of geopolymer concrete (GPC) to sustain the temperature and relative humidity according to Amleh et al.[5].
- Galvanized steel or stainless steel rebars should be utilized instead of carbon steel rebars to inhibit the corrosion of steel rebars. Moreover, the combination of corrosion-resistant nickel with oxidation-resistant chromium yields an alloy suitable for use in both oxidizing and reducing chemical environments.

- Utilizing geopolymer concrete (GPC) made of sustainable materials instead of normal concrete for RC members exposed to extreme environmental conditions to increase the service life and durability of the RC structures, according to Amleh et al.[5].
- Precursor Materials like FA and SG in GPC exhibit high durability, improved strength, and greater resistance to high temperatures and chloride penetration [29-35].
- Increasing the concrete cover to at least 50 mm for RC members made of GPC would lead to a significant reduction in the probability of corrosion at low and intermediate temperature levels, according to Amlehet al. [5].
- Using calcium nitrite-based corrosion inhibitors associated with the optimum percentage of FA (approximately 20%).

This manuscript thoroughly investigates the effects of climate change on infrastructure, with a specific focus on the potential for chloride-induced corrosion initiation in North American infrastructure. A detailed mechanistic probabilistic model was conducted using Monte Carlo simulation across diverse RCP scenarios. The findings can inform urban planning, influence construction choices, and shape safety standards, potentially offering economic advantages by minimizing repair expenses and bolstering community safety. The importance of this study lies in offering a model that can be applied globally, emphasizing the importance of robust urban infrastructure in the face of climate challenges.

2. Research Methodology

This methodology provides a comprehensive, data-driven, and statistically robust framework for determining and predicting the impact of climatic changes on the structural integrity of RC structures, with a specific focus on Toronto's urban environment. This study utilizes a Monte-Carlo simulation method to determine the probability of corrosion initiation (PCI) for RC structures at different RCPs, which reflect potential future greenhouse gas emission scenarios, converging upon the envisioned climatic trajectory for the projected maximum temperature in the future for Toronto city. Focusing on two distinct RCPs (RCP2.6 and RCP8.5) and several concrete covers ranging from 30 mm to 70 mm. In addition, the PCI will be conducted across different chloride concentrations (6, 8, 10, 12, 14, 16, and 18 kg/m^3) at different timelines, using the following steps:

1-Data Collection and Calculation: In this study, the projected maximum temperature data across different RCPs, especially RCP2.6 and RCP8.5, for Toronto City will be collected annually starting from the year 2000 till the year 2100 to see the trend of the levels in the future. The relative humidity will be assumed in most cases to be equal to 65% and 70%. The average diffusion coefficient over time and the chloride concentration data will be determined through detailed calculations.

2-Monte-Carlo Simulation Model Development: The Monte-Carlo simulation model will be developed to predict the PCI for RC structures. The model will consider the impact of various projected maximum temperature levels in the future across various RCPs, concrete covers, chloride concentrations, diffusion coefficients, and time. The model will use the collected and calculated data to simulate different scenarios and predict the PCI for each scenario.

3-Simulation Process and Iteration: The Monte Carlo simulation process will be conducted to generate random samples from the input distributions. The model will then calculate the predicted PCI for each sample, and the simulation will repeat this process 100,000 times to generate an accurate result, ultimately enabling a comprehensive investigation of potential outcomes.

4-Analytical Evaluation: The results of the Monte-Carlo simulation will be analyzed to determine the PCI for each scenario. The analysis will include statistical measures such as the mean, standard deviation, coefficient of variation, and distribution for each random variable.

Chloride Penetration Depth Model: Considering Environmental Factors

For the initial condition C_f (d>0, t=0) =0 and boundary condition C_f (d=0, t>0) =constant, an equation for the conduction of the free chloride concentration can be obtained as shown in equation (9).

$$C_f(d,t) = C_o^f \left[1 - \text{erf}\left(\frac{d}{2\sqrt{D_a \times t}}\right)\right] \quad (9)$$

Where: C_f(d,t) is the chloride concentration (kg/m^3) at depth (x) and time (t);C_o^f is the surface content of free chloride (kg/m^3).D_a is the apparent chloride diffusion coefficient (m^2/s), and d is the concrete cover thickness (m).

Chloride Ingress Modeling: The chloride ingress into RC structures due to de-icing salts is transported by severalmechanisms, such as water surface absorption in partially saturated concrete and ionic diffusion in saturated concrete. In modeling chloride transport to the steel rebars embedded inside concrete, the process of ionic diffusion is considered.

2.1. Calculation of The Average Chloride Diffusion Coefficient for Various Types of Concrete

Over time, the average chloride diffusion coefficient is an essential parameter for estimating the service life of RC structures exposed to severe environmental conditions. The reference chloride diffusion coefficient (D_{ref}) is a constant value, calculated using equation (10) according to Bentz and Thomas [36], who proposed a relationship between $D_{ref}$and the water-to-cement ratio (W/C) of concrete.

$D_{ref}=10^{(-12.06+2.4\ W/C)}$ (10)

Where: Dref is the reference chloride diffusion coefficient (m^2/s), and W/C is the water-to-cement ratio used in the concrete mix.

The formula used to account for the age factors (m) that describe the percentages of SCMs (e.g., specific percentages of FA up to 50% or SG up to 70%) used as a partial replacement with the total amount of cement used in the concrete mixes depending on mix proportions is expressed as in equation (11) according to Bentz and Thomas, [36].

$m = 0.2 + 0.4(\%FA/50 + \%SG/70)$ (11)

Where m is a constant representing the age factor depending on the percentage of either FA (%FA) or SG (%SG), or a combination of both, used partially to replace the total cement used in the concrete mix.

The average chloride diffusion coefficient (D_m) at a particular time (t) (m^2/s) is calculated using equations (12) and (13).

$$D_m = \frac{D_{ref}}{1-m}\left(\frac{t_{ref}}{t}\right)^m \qquad t < t_R \quad (12)$$

$$D_m = D_{ref}\left[1 + \left(\frac{t_R}{t} \times \frac{m}{1-m}\right)\right]\left(\frac{t_{ref}}{t_R}\right)^m \qquad t \geq t_R \quad (13)$$

Where t_R=30 years, t_{ref}=28 days, D_m is the average chloride diffusion coefficient at a particular time (m^2/s), and (t) is time (years).

Figure 1illustrates the decreasing trend in the average chloride diffusion coefficients over time. Both FA and SG concrete demonstrate improved resistance against chloride ions, often with average diffusion coefficients falling below 10^{-12} m^2/s. In later exposure stages, FA can significantly decrease the diffusion rate of chloride ions in concrete. FA decreases the diffusion coefficient of chloride ions by 15%–50% according to Oh and Jang [37], thereby extending the expected service life of concrete structures. The results indicate that a combined mix containing an optimal percentage of FA and SG, specifically (50% FA and 50% SG) as shown in Figure 1, leads to lower average chloride diffusion coefficients over time compared to the mix that incorporates 0% FA and 0% SG. Therefore, the mix that contains 50% FA and 50% SG reduces the average chloride diffusion coefficients by a range varying from 1/4 to 1/19 times the average diffusion coefficients from mixes that do not incorporate these proportions of FA and SG, as shown in Figure 1. This research sets the water-to-cement ratio at 0.4 to assess the probability of chloride-induced corrosion initiation at different relative humidity levels in various future years.

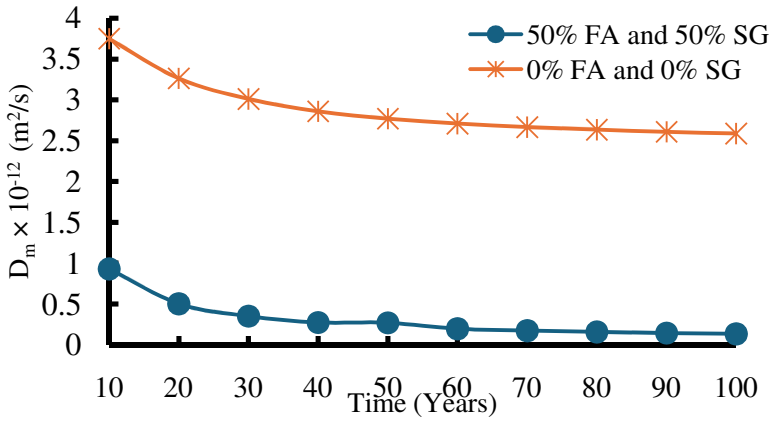

Figure 1. Average chloride diffusion coefficient (D_m) values across various years for two different concrete mixes.

2.2.Performance Function (PF) For the Chloride-Induced Corrosion for Uncracked and Cracked Concrete Sections

Considering the uncertainties in chloride concentration prediction, the Monte Carlo simulation (MCS) method is the most widely used approach. The C_o prediction encompasses various uncertainties, including statistical, physical, decisional, and model uncertainties. The probability of corrosion can be estimated using various reliability methods as follows:

$$\text{Methods for Predicting the Probability of Corrosion} \begin{cases} \text{MCS Method} \\ \text{First Order Reliability Method (FORM)} \\ \text{Second} - \text{Order Reliability Method (SORM)} \\ \text{Advanced First Order Reliability Method} \end{cases}$$

For a prescribed PF(g) is the difference between a term that is equivalent to a resistance and a term that is equivalent to a load effect, expressed as shown in equation (14). The term resistance can be used to refer to the chloride threshold level, which defines the resistance of the concrete cover to corrosion-induced cracks, spalling, or delamination. Similarly, the term load effect refers to the chloride concentration at the steel level, spalling, etc. The probability of failure is equal to the area of the frequency distribution for which $g < 0$, where gis calculated using random values of R and Q.

$$g=R-Q \quad (14)$$

Therefore, the PF for corrosion initiation due to chlorides can be formulated as a function of four variables, as in equations (15) and (16).

$$g(C_o, d, D, C_{th}) = C_{th} - C_{d,t}(C_o, d, D, t) \quad (15)$$

$$g(C_s, d, D, C_{th}) = C_{th} - C_o\left(1 - \text{erf}\left(\frac{d}{2 \times \sqrt{D \times t}}\right)\right) \quad (16)$$

3. Analysis of Results

3.1. Validation of the Chloride-Induced Corrosion Initiation Model

The proposed probabilistic approach aims to predict the probability of chloride-induced corrosion initiation over time at various relative humidity levels and concrete cover depths. Its application is demonstrated on a real RC deck of a highway bridge exposed to de-icing salts. The input parameters are sourced from field data, as documented by Saassouh and Lounis [38], and are summarized in Table 3. The table elaborates on the statistical mean, coefficient of variation, and distribution of different random variables, including C_{th}, C_o, and d.

Table 3. The mean and coefficient of variation for different random variables for RC bridges subjected to chlorides.

Random Variables	Mean Value (μ)	Coefficient of Variation (COV)	Distribution
Chloride Concentration (C_o) (kg/m^3)	6	30%	Log-normal
Concrete Cover (d) (mm)	70	20%	

Chloride threshold (C_{th}) (kg/m^3)	0.7	20%	

Saassouh and Lounis [38] conducted projections of the probability of corrosion initiation for the RC bridge deck member subjected to deicing salts using Monte Carlo simulation (MCS) at every interval of time. Moreover, all the random variables, including concrete cover (d), chloride concentration (C_o), and chloride threshold (C_{th}), were assumed to follow a lognormal distribution. Saassouh and Lounis [38] found that the probability of corrosion initiation at a specific time, especially at 23 years and 10 months, was around 45%. The current model is compared with the results obtained by Saassouh and Lounis [38] for the RC bridge deck data mentioned in Table 3 using the MCS consisting of 100,000 simulations, and it was found that the results of the current model coincide with the results conducted by Saassouh and Lounis [38].

3.2. Interaction Between Relative Humidity, Concrete Cover, and Probabilities of Chloride-Induced Corrosion for Various RCP Scenarios

The MCS method, utilizing 100,000 samples, provided a thorough analysis of the probability of chloride-induced corrosion initiation under varying conditions. This included multiple concrete covers ranging from 30 to 70 mm in this case, evaluated at different RCPs for the projected maximum temperature for Toronto city, and two relative humidity levels (RH=65% and RH=70%) to deduce a comparison between the values of the PCI obtained for the corresponding RH=70% and the PCI obtained for the corresponding RH= 65%. For consistency in comparison, the average diffusion coefficient (D_m) remained fixed at a W/C ratio of 0.4. Meanwhile, the chloride concentration (C_o) was set at 6 kg/m^3, while the chloride threshold (C_{th}) was established at 0.7 kg/m^3.

Key Observations:

• For a concrete cover (CV) of 30 mm and RH=65%, the PCI values were found to be 51% and 74% for RCP2.6 and RCP8.5, respectively (see Figure 2 and Table 4).

• An increase in relative humidity to 70% at a CV of 30 mm led to a rise in PCI to 84% and 95% for RCP2.6 and RCP8.5, respectively (see Figure 3 and Table 4).

• As the CV increased to 70 mm, there was a marked reduction in PCI across all RCPs and humidity levels, confirming the protective effect of a thicker concrete layer.

• There was a substantial decrease in PCI as CV changed from 30 mm to 70 mm: from (51% to 0.01%) and from (74% to 0.1%) for RCP2.6 and RCP8.5, respectively, at RH=65% and from 84% to 0.3% and from 95% to 2% for RCP2.6 and RCP8.5, respectively, at RH=70%.

Table 4. Probability of chloride-induced corrosion initiation across various concrete covers, relative humidity levels at different RCPs in 100 years of chloride exposure.

Concrete Cover (CV) (mm)	**RH=65%**		**RH=70%**	
	RCP2.6	**RCP8.5**	**RCP2.6**	**RCP8.5**
30	51%	74%	84%	95%
40	11%	27%	40%	65%
50	1%	6%	11%	28%
60	0.10%	0.80%	2%	8%
70	0.01%	0.10%	0.3%	2%

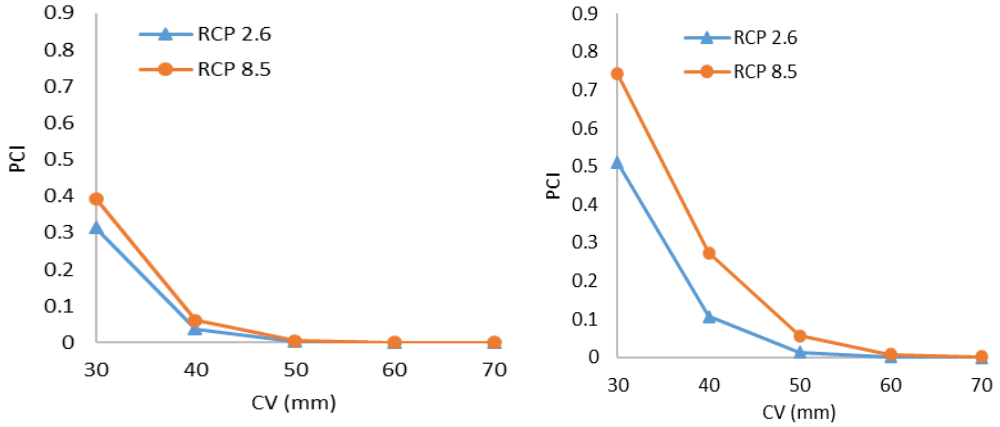

(a) (b)

Figure 2. Influence of different concrete covers on the corresponding PCI in different years, considering RH=65% impacting the chloride diffusion coefficient: (a) Year 50, (b) Year 100.

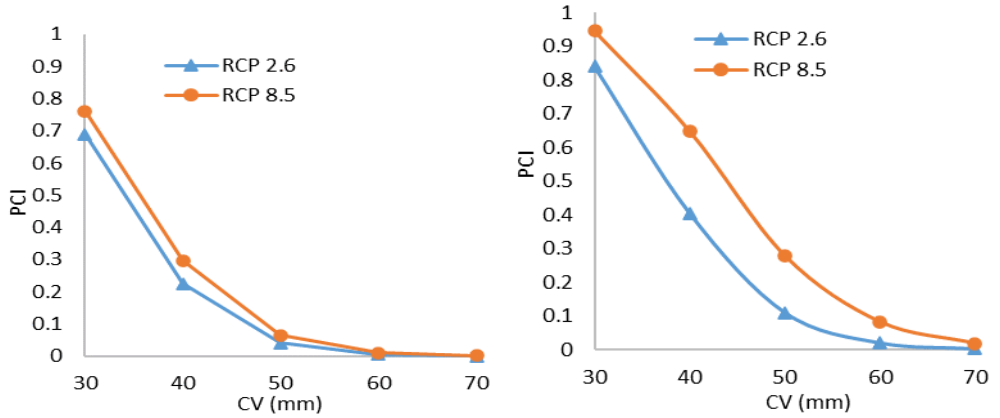

(a) (b)

Figure 3. Influence of different concrete covers on the corresponding PCI in other years, considering RH=70% impacting the chloride diffusion coefficient: (a) Year 50, (b) Year 100.

This analysis highlights the significance of concrete cover thickness and relative humidity in influencing the probability of chloride-induced corrosion, especially in varied climatic scenarios represented by RCPs.

3.3. Impact of Varying Chloride Concentrations on the PCI across Diverse Concrete Covers

The study examined the consequences of fluctuating chloride concentrations on the PCI for a concrete mixture containing 460 kg/m^3 of cement within the structural framework of RC. Again, this evaluation utilized MCS with a sample size of 100,000. With the W/C ratio set at 0.4, the average diffusion coefficient (D_m) was determined. The chloride threshold was capped at 0.15% of the weight of the cement in line with the CSA A23.1-14 standards, as shown in Table 5. There is a huge variability in the surface chloride concentration applied on the RC bridge deck between one region and another; it can vary from 0 to 25 kg/m^3. The chloride concentrations (C_o) applied to the RC deck's surface ranged from 6 to 18 kg/m^3, which is linked to the use of de-icing salts, as shown in Table 5. A constant relative humidity of 70% was maintained throughout this scenario.

Table 5.Mean (μ) and coefficient of variation (COV) values for the chloride threshold (C_{th}) and chloride concentration (C_o).

Random Variables	Values
Mean for chloride threshold (C_{th}) (kg/m^3)	0.15% of the weight of the cement (CSA A23.1-14)
Mean (μ)	(0.7 kg/m^3)
COV for (C_{th})	20%
Distribution for (C_{th})	Log-normal Distribution
Chloride Concentration (C_o)	Range (6-18) (kg/m^3)
COV for (C_o)	30%
Distribution for (C_o)	Log-normal Distribution

For a 40 mm concrete cover and a 6 kg/m^3 of chloride concentration, the computed PCI values for RCP2.6 and RCP8.5 stood at 41% and 65%, respectively, for a 100-year timeline, for a chloride concentration equal to 6 kg/m^3, as illustrated in Table 6. However, a rise in the CV to 60 mm witnessed a sharp reduction in PCI values to 2% and 8% for the respective RCP scenarios, as shown in Table 6.

With a higher chloride concentration of 10 kg/m^3, at a CV of 40 mm, the PCI rose to 67% for RCP2.6 and 86% for RCP8.5. A subsequent increment of the CV to 60 mm reflected a sharp drop in PCI values, settling at 8% for RCP2.6 and 22% for RCP8.5, as shown in Table 6. Progressing with a chloride concentration of 18 kg/m^3, the PCIs reached 86% and 96% for the two RCP scenarios at CV=40 mm, as shown in Table 6. This trend reversed with a CV increase to 60 mm, culminating in PCI values of 20% and 43% for RCP2.6 and RCP8.5, respectively, as illustrated in Table 6.

Table 6 illustrates the increase in the PCI when the chloride concentration changed from 6 to 18 kg/m^3 across various RCP scenarios and concrete covers. In-depth data analysis indicated that the PCI changed significantly from 41% to 86% for RCP2.6 and from 65% to 96% for RCP8.5, when the C_o changed from 6 to 18 kg/m^3, at a CV equal to 40 mm. Concrete cover requirements across chloride concentrations and RCP scenarios for 50- and 100-year projections are detailed in Table 6. Moreover, the PCI increased from 2% to 20% and from 8% to 43% for RCP2.6 and RCP8.5, respectively, when the chloride concentration changed from 6 to 18 kg/m^3, when a CV equals to 60 mm.

Table 6. Probability of chloride-induced corrosion initiation at different CVs and C_o values across various RCPs at T=100 years of chloride exposure.

	C_o=6 kg/m^3		**C_o=10 kg/m^3**		**C_o=18 kg/m^3**	
(CV) (mm)	**RCP2.6**	**RCP8.5**	**RCP2.6**	**RCP8.5**	**RCP2.6**	**RCP8.5**
40	41%	65%	67%	86%	86%	96%
60	2%	8%	8%	22%	20%	43%

The influence of various chloride concentrations on the PCI is deduced from Figure 4, considering the highest and lowest emission scenarios (RCP2.6 and RCP8.5) at multiple years for CVs equal to 40 mm and 60 mm, and distinctly captures the influence of varying chloride concentrations on the PCI. It is evident that RCP8.5's PCI, when taking a concrete cover of 40 mm, consistently surpasses that of a concrete cover of 60 mm. Furthermore, for RCP8.5 at a 50-year marker, the PCI increased by approximately a range of 50% to 60% as the chloride concentration changed from 6 kg/m^3 to 18 kg/m^3, as shown in Figure 4 (a). However, as the concrete cover increased to 60 mm, the change in the PCI isn't significant (i.e., low impact on PCI) as the chloride concentration varied from 6 kg/m^3 to 18 kg/m^3 at 50 years of chloride exposure (see Figure 4 (a)). Finally, it was noticed that the values of the PCI at 100 years of exposure to concrete covers of either 40 mm or 60 mm used in RC decks across various RCPs

are significantly higher than their values at 50 years of chloride exposure (see Figure 4 (b)) at different chloride concentrations.

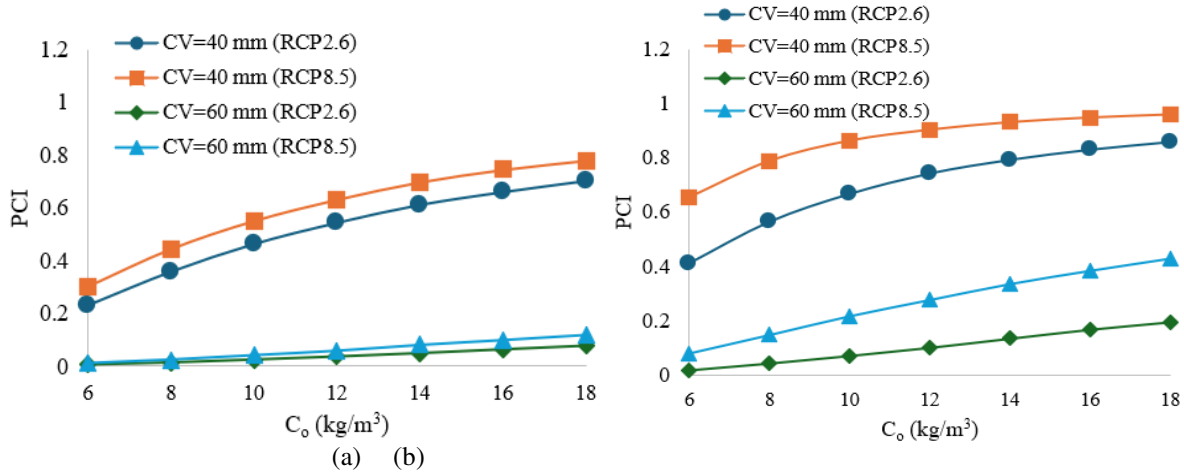

Figure 4.Projection of the PCIs across different chloride concentrations, RCPs, and concrete covers in various years: (a) Year 50, (b) Year 100.

4. CONCLUSION

The urban landscape of certain cities in Ontario province, susceptible to the severe forces of varied climate change impacts. Utilizing the Monte Carlo simulation across diverse RCPs to gauge the consequences of climate change on the likelihood of chloride-induced corrosion initiation within the confines of Toronto City. The concrete mix used for the deck of the RC bridge contains an optimal percentage of FA and SG, specifically (50% FA and 50% SG), which leads to lower average chloride diffusion coefficients by a range of 1/4 to 1/19 over time compared to the average chloride diffusion coefficients for the corresponding concrete mix that doesn't includes any percentages of SCMs to conduct the PCI. In addition, the water-to-cement ratio used in the concrete mix is set at 0.4. Moreover, the corrected chloride diffusion coefficient used in the performance function considered the impact of the maximum temperature, maturation time of concrete, and relative humidity to conduct the PCI over time.

The primary conclusions drawn from our analysis are:

1) The projections of the PCIs reached maximum values at concrete covers of 30 mm and 40 mm at different RCPs and RH%, including (65% and 70%), in various future years.
2) There was a marked decrease in PCI as CV changed from 30 mm to 70 mm for the lowest and highest emission scenarios of maximum temperature, at RH=65% and 70%. Therefore, as the CV increased to 70 mm or beyond, there was a marked reduction in PCI across various RCPs and relative humidity levels, confirming the protective effect of a thicker concrete cover for the RC members.
3) Chloride Concentration's Role in Corrosion Dynamics: The study reveals that chloride concentrations significantly influence corrosion initiation probabilities. The increase of the chloride concentrations from 6 kg/m^3 to 18 kg/m^3 applied on the RC deck leads to a significant increase of the PCI values from (65% to 96%) and (8.2% to 43%) for the following concrete covers of 40 mm and 60 mm, respectively, for the high emission scenario (RCP8.5) in year 100. The second-degree polynomial function relationship between projected PCI values and distinct chloride concentrations for concrete covers of 40 and 60 mm is deduced in this research in chloride-rich environments applied on the top part of the RC deck.
4) More sustainable construction materials, instead of FA and SG, should be adopted in the future for use in the members subjected to extreme chloride environments, accompanied by extreme climate change, to further enhance the resilience of infrastructure.

Limitations and Recommendations: The relative humidity used in this research is set at 70% in most cases to conduct the PCI, while the comparison study was conducted to see the impact of two relative humidity levels on the PCI were set at 65% and 70%. The external chloride concentration applied to the surface of the RC bridge deck, which ranged from 6 to 18 kg/m^3, is related to the use of deicing salts on the RC bridge deck. According to the results, this research recommends increasing the concrete cover for the new and existing RC bridge decks in Ontario province by a minimum value of 70 mm instead of 30 mm and 40 mm to successfully resist the effect of deicing salts and the increase in the maximum temperature levels in the future across various emission scenarios. The

limitation of this research should be extended to the uncertainties in climate projections, variability in field conditions (e.g., cracks, workmanship, etc.), and the assumption related to FA and SG proportions in the concrete mix and its variability.

This research is a wake-up call for engineers, urban planners, and policymakers in Toronto and beyond. There's a pressing need to recalibrate construction standards, material choices, and maintenance regimes in alignment with the insights from such studies. The connection between climate change, material science, and urban infrastructure warrants a multidisciplinary approach, and this manuscript is a stepping-stone in that overarching journey. Finally, maintenance optimization models should be developed so that decision-makers can take quick actions regarding retrofitting RC structure members that are subjected to extreme climate change.

References

[1] Hassan, M. (2025). Evaluating the Durability of RC Bridges Under Climate Scenarios: A Study of Carbonation and Chloride-induced Corrosion. PhD Thesis, Department of Civil Engineering, Toronto Metropolitan University, Toronto, Ontario, Canada.https://doi.org/10.32920/30581534.v1

[2] Hassan, M., and Amleh, L. (2024). Influence of Climate Change on Probability of Carbonation-Induced Corrosion Initiation. PeriodicaPolytechnica Civil Engineering Journal, 68 (1): 57-67. https://doi.org/10.3311/PPci.22101

[3] Hassan, M., and Amleh, L. (2025). Influence of Various Crack Widths in RC Bridge Decks on the Initiation of Chloride-Induced Corrosion. Journal of Composites Science, 9, 242. https://doi.org/10.3390/jcs9050242

[4] Hassan, M.; L. Amleh; and L. Hussein. (2024). Projection of the Carbonation Depths and its Probability of Corrosion Initiation for the Uncracked and Cracked Concrete. International Review of Civil Engineering (IRECE), 15 (5): 381-398. https://doi.org/10.15866/irece.v15i5.24986

[5] Amleh, L.; M. Hassan; and L. Hussein. (2024). Influence of Climate Change on the Probability of Chloride-Induced Corrosion Initiation for RC Bridge Decks Made of Geopolymer Concrete. Sustainability, 16, 8200. https://doi.org/10.3390/su16188200

[6] Hassan, M.; L. Amleh; and H. Othman. (2022). Effect of Different Cement Content and Water-Cement Ratio on Carbonation Depth and Probability of Carbonation-Induced Corrosion for Concrete. Cement Wapno Beton, 27 (2): 126-143. https://doi.org/10.32047/cwb.2022.27.2.4

[7] Hassan,M.(2025). Assessment of Temperature Levels on the Probability of Corrosion for RC Decks Made of Various Percentages of Supplementary Cementitious Materials, SSRG International Journal of Civil Engineering, 12 (11): 36-54.https://doi.org/10.14445/23488352/IJCE-V12I11P104

[8] Hassaan, M.; M.I. Elmasry; and N.E. Ashkar.(2021).Structural Health Monitoring for Reinforced Concrete Containment Using Inner Electrical Resistivity Method. Open Journal of Civil Engineering, 11(3): 317-341. https://doi.org/10.4236/ojce.2021.113019

[9] Hassaan, M.; M.I. Elmasry; and N.E. Ashkar. (2021). Detection of Cracks in Heavy-Weight Concrete Using Inner Electrical Resistivity Method. Saudi Journal of Civil Engineering, 5(9): 355-366. https://doi.org/10.36348/sjce.2021.v05i09.004

[10] Hassaan, M.; M.I. Elmasry; and N.E. Ashkar.(2021). Effect of Impact Boeing 707-320 on External RC Containment of Nuclear Power Plant for Different Compressive Strength of Concrete. Saudi Journal of Civil Engineering, 5(8): 282-304. https://doi.org/10.36348/sjce.2021.v05i08.004

[11] Qu, F.; J. Zhang; G. Liu; and S. Zhao. (2022). Experimental Study on Chloride Ion Diffusion in Concrete Affected by Exposure Conditions, Materials, 15, 2917.https://doi.org/10.3390/ma15082917

[12] Melchers, R.E.; Chaves, I.A.(2021). Durable Steel-Reinforced Concrete Structures for Marine Environments. Sustainability, 13, 13695.https://doi.org/10.3390/su132413695

[13] Lee, S.A.; K.P. Park; J. Kim; K.Y. Ann.(2020). Sensitivity analysis for binders in concrete mix to the corrosion risk of steel embedment in chloride-bearing environments. Construction and Building Materials, 251, 118944, ISSN 0950-0618.https://doi.org/10.1016/j.conbuildmat.2020.118944.

[14] Thomas, M.D.A., and Bamforth, P.B.(1999).Modelling chloride diffusion in concrete: Effect of fly ash and slag. Cement and Concrete Research, 29 (4): 487-495, ISSN 0008-8846.https://doi.org/10.1016/S0008-8846(98)00192-6

[15] Engelund, S.; C. Edvardsen; and L. Mohr. (2000). General guidelines for durability design and redesign. Report R15 of EU-Brite EuRam III project BE95-1347 DuraCrete, Probabilistic performance-based durability design of concrete structures.

[16] De Weerdt, K.(2021). Chloride binding in concrete: recent investigations and recognised knowledge gaps: RILEM Robert L'Hermite Medal Paper 2021. Materials and Structures, 54, 214.https://doi.org/10.1617/s11527-021-01793-9

[17] Page, C.L.; N.R. Short; and A. El Tarras. (1981). Diffusion of chloride ions in hardened cement pastes. Cement and Concrete Research, 11(3): 395–406.https://doi.org/10.1016/0008-8846(81)90111-3

[18] Bazant, Z.P., and Najjar, L.J. (1971). Drying of concrete as a nonlinear diffusion problem. Cement and Concrete Research,1 (5): 461–473.https://doi.org/10.1016/0008-8846(71)90054-8
[19] Rincon, L.F.; Y.M. Moscoso; A.E.A. Hamami; J.C. Matos; E. Bastidas-Arteaga. (2024).Degradation Models and Maintenance Strategies for Reinforced Concrete Structures in Coastal Environments under Climate Change: A Review. Buildings, 14, 562.https://doi.org/10.3390/buildings14030562
[20] Lounis, Z., and Daigle, L. (2008). Reliability-based decision support tool for life cycle design and management of highway bridge decks. Annual Conference of the Transportation Association of Canada, Toronto, Ontario, 1-19.
[21] Zhao, J.; E.D. Shumuye; and Z. Wang. (2021). Effect of Slag Cement on Concrete Resistance Against Combined Exposure to Freeze-Thaw and Chloride Ingress. Journal of Engineering Science and Technology, 16 (6): 4687 – 4706.
[22] Liu, J.; J. Liu; Z. Huang; J. Zhu; W. Liu; and W. Zhang. (2020). Effect of Fly Ash as Cement Replacement on Chloride Diffusion. Chloride Binding Capacity and Micro-Properties of Concrete in a Water Soaking Environment. Applied Sciences, 10(18), 6271.https://doi.org/10.3390/app10186271
[23] Adiyastuti, S.M.; B. Iqbal; and E.C. Ilman. (2024). Effect of cracking in fly ash concrete on chloride diffusion rate. IOP Conference Series: Earth and Environmental Science, 1464, 012030. https://doi.org/10.1088/1755-1315/1464/1/012030
[24] Zhang, J.; Zhou, X.-Z.; Zheng, J.-J.; Ye, H.-L.; Yang, J.(2020).Experimental Investigation and Analytical Modeling of Chloride Diffusivity of Fly Ash Concrete. Materials, 13, 862.https://doi.org/10.3390/ma13040862
[25] Ampadu, K.O.; K. Torii; and M. Kawamura. (1999). Beneficial effect of fly ash on chloride diffusivity of hardened cement paste. Cement and Concrete Research, 29 (4): 585-590, ISSN 0008-8846.https://doi.org/10.1016/S0008-8846(99)00047-2
[26] Bentz, D.P.; O. M. Jensen; A.M. Coats; and F.P. Glasser. (2000). Influence of silica fume on diffusivity in cement-based materials. I. Experimental and computer modeling studies on cement pastes. Cement and Concrete Research, 30 (6): 953-962. https://doi.org/10.1016/S0008-8846(00)00264-7
[27] Ahmad, S.; O.S.B. Al-Amoudi; S.M.S. Khan; M. Maslehuddin.(2022). Effect of silica fume inclusion on the strength, shrinkage, and durability characteristics of natural pozzolan-based cement concrete. Case Studies in Construction Materials, 17, e01255, ISSN 2214-5095. https://doi.org/10.1016/j.cscm.2022.e01255.
[28] Correia, V.; J. Gomes Ferreira; L. Tang; and A. Lindvall. (2020).Effect of the Addition of GGBS on the Frost Scaling and Chloride Migration Resistance of Concrete. Applied Sciences, 10, 3940.https://doi.org/10.3390/app10113940
[29] Amran, Y.M.; R. Alyousef; H. Alabduljabbar; and M. El-Zeadani. (2020). Clean production and properties of geopolymer concrete, a review. Journal of Cleaner Production, 251, Article 119679. https://doi.org/10.1016/j.jclepro.2019.119679
[30] Amran, M.; S. Debbarma; and T. Ozbakkaloglu. (2021). Fly ash-based eco-friendly geopolymer concrete: A critical review of the long-term durability properties. Construction and Building Materials, 270 (8), ISSN 0950-0618. https://doi.org/10.1016/j.conbuildmat.2020.121857
[31] Sbahieh, S.; G. McKay; and S.G. Al-Ghamdi. (2023).Comprehensive Analysis of Geopolymer Materials: Properties, Environmental Impacts, and Applications. Materials, 16, 7363.https://doi.org/10.3390/ma16237363
[32] Shehata, N.; O.A. Mohamed; E.T. Sayed; M.A. Abdelkareem; and A.G. Olabi. (2022). Geopolymer concrete as green building materials: Recent applications. Sustainable development and circular economy potentials. Science of The Total Environment, 836, 155577. https://doi.org/10.1016/j.scitotenv.2022.155577
[33] Shehata, N.; E.T. Sayed; and M.A. Abdelkareem. (2021).Recent Progress in Environmentally Friendly Geopolymers: A Review. Science of the Total Environment, 762, 143166, ISSN 0048-9697.https://doi.org/10.1016/j.scitotenv.2020.143166
[34] Bajpai, R.; K. Choudhary; A. Srivastava; K.S. Sangwan; and M. Singh. (2020).Environmental impact assessment of fly ash and silica fume-based geopolymer concrete. Journal of Cleaner Production, 254, 120147, ISSN 0959-6526. https://doi.org/10.1016/j.jclepro.2020.120147
[35] Firdous, R.; M. Nikravan; and R. Mancke. (2022). Assessment of environmental, economic, and technical performance of geopolymer concrete: a case study. Journal of Materials Science, 57: 18711–18725.https://doi.org/10.1007/s10853-022-07820-6
[36] Bentz, E.C., and Thomas, M.D.A. (2013). Life-365 service life prediction model, Life-365 Consortium III. The Silica Fume Association, Lovettsville, VA.
[37] Oh, B.H., and Jang, S.Y.(2007). Effects of Material and Environmental Parameters on Chloride Penetration Profiles in Concrete Structures. Cement and Concrete Research, 37 (1): 47–53.https://doi.org/10.1016/j.cemconres.2006.09.005

[38]Saassouh, B.; and Lounis, Z.(2012). Probabilistic modeling of chloride-induced corrosion in concrete structures using first- and second-order reliability methods. Cement and Concrete Composites, 34: 1082-1093.https://doi.org/10.1016/j.cemconcomp.2012.05.001